Biochemical Engineering Journal 63 (2012) 116–123

Contents lists available at SciVerse ScienceDirect

Biochemical Engineering Journal

journal homepage: www.elsevier.com/locate/bej

Review

On the Lambert *W* function and its utility in biochemical kinetics

Marko Goličnik*

Institute of Biochemistry, Faculty of Medicine, University of Ljubljana, Vrazov trg 2, 1000 Ljubljana, Slovenia

ARTICLE INFO

Article history:
Received 6 October 2011
Received in revised form
20 December 2011
Accepted 21 January 2012
Available online 3 February 2012

Keywords:
Biokinetics
Biosensors
Enzymes
Integrated rate equation
Kinetic parameters
Lambert *W* function

ABSTRACT

This article presents closed-form analytic solutions to three illustrative problems in biochemical kinetics that have usually been considered solvable only by various numerical methods. The problems solved concern two enzyme-catalyzed reaction systems that obey diversely modified Michaelis–Menten rate equations, and biomolecule surface binding that is limited by mass transport. These problems involve the solutions of transcendental equations that include products of variables and their logarithms. Such equations are solvable by the use of the Lambert $W(x)$ function. Thus, these standard kinetics examples are solved in terms of $W(x)$ to show the applicability of this commonly unknown function to the biochemical community. Hence, this review first of all describes the mathematical definition and properties of the $W(x)$ function and its numerical evaluations, together with analytical approximations, and then it describes the use of the $W(x)$ function in biochemical kinetics. Other applications of the function in various engineering sciences are also cited, although not described.

Contents

1. Introduction

A function that is convenient for solving transcendental equations of the type $y + \ln(y) = x$ was derived and used independently by several researchers [1–3] before Corless et al. settled on a common notation in the mid-1990s [4,5]. They called it the Lambert *W* function (the letter *W* was chosen following the use of early Maple software [4]), on the consideration that this function can be traced back to Johann Lambert in around 1758, and it was considered later by Leonhard Euler [for references, see 5]. These two mathematicians developed a series solution for the trinomial equation, although they left it unnamed. However, in the years during the Lambert/Euler era and through the modern history of Maple [4], this function did not disappear entirely, even if the literature remained widely scattered and obscure until the function acquired the name of the Lambert *W* function. Meanwhile, Wright [1] analyzed the solution of the equation $z\exp(z) = a$, in 1959, and later, in 1973, Fritsch et al. [2] presented an efficient algorithm for the root computation of such nonlinear transcendental equations. However,

* Tel.: +386 1 5437669; fax: +386 1 5437641.
E-mail address: marko.golicnik@mf.uni-lj.si

1369-703X/$ – see front matter © 2012 Elsevier B.V. All rights reserved.
doi:10.1016/j.bej.2012.01.010

even a decade later, in the early 1980s, Beal still evaluated the solutions to the Michaelis–Menten equation using either a table for the so-called function '*F*' [3] or a relatively slow Newton's root-finding method [6].

However, across numerous scientific disciplines, the modern knowledge of the Lambert *W* function as a mathematical tool has allowed the derivation of closed-form solutions for models for which explicit or exact solutions were not known, and therefore where alternative iterative methods or approximate solutions had been used. Thus the Lambert *W* function can arise in a wide scope of practical problems in mathematics, computer science [5], mathematical physics [5,7] and engineering (see [8] and references therein), although it received little attention in biochemistry and biotechnology. In these latter disciplines, the solutions to relatively simple model equations are frequently given by a standard family of transcendental equations of the following type:

$$A \cdot y + \ln(B + C \cdot y) = \ln(D) \tag{1}$$

where *A*, *B*, *C* and *D* do not depend on *y*. For many life scientists that are faced with Eq. (1) in this implicit form, the usual next step is to search for an available and efficient root-finding computer algorithm that can numerically evaluate the dependent variable *y*. Thus, they are not aware that Eq. (1) has the solution as given in its closed form:

$$y = \frac{1}{A} \cdot W\left(\frac{A \cdot D}{C} \cdot \exp\left(\frac{A \cdot B}{C}\right)\right) - \frac{B}{C} \tag{2}$$

where *W* stands for the Lambert *W* function. Therefore, I believe that it is expedient to illustrate here this function and how to use it in practice. This is the subject of the present article, in which examples of specific biochemical kinetics are given that can be solved algebraically and expressed in the closed form only in terms of the Lambert *W* function. Other applications of the use of the Lambert *W* function in various engineering disciplines are also cited at the end of this review, although these are not described in detail.

2. Mathematical properties of the Lambert *W* function

The Lambert *W* function is defined as the solution to the following transcendental equation:

$$y \cdot exp(y) = x \tag{3}$$

although using a logarithmic transformation, Eq. (3) can also be rewritten as:

$$y + \ln(y) = \ln(x) \tag{4}$$

However, the solution to Eqs. (3) and (4) is the Lambert *W* function, and it is written as:

$$y = W(x) \tag{5}$$

Actually, when *x* is a general complex number, there are an infinite number of solution branches that can be labeled with an integer subscript, as $W_k(x)$ for $k = 0, \pm1, \pm2, \ldots$. However, if *x* is a real number, the only two branches that take on real values are $W_0(x)$ and $W_{-1}(x)$. This function is real valued for the interval $[-\exp(-1),\infty)$ where it takes on values from $-\infty$ to ∞, although it is two valued for negative *x*. As can be seen in Fig. 1, a branching point located at $(-\exp(-1),-1)$ separates the two branches of the Lambert *W* function; i.e. the upper branch, $W_0(x)$, and the lower branch, $W_{-1}(x)$. These two branches are the only ones that are needed in the applications of this article, although for practical reasons, $W_0(x)$ is frequently separated into two regions for positive and negative argument *x* (see Fig. 1). Both of these branches have a common vertical tangent at the branching point. The upper branch, $W_0(x)$, is usually called the principal branch: it passes through the coordinate origin, as for the lower branch $W_{-1}(x)$, and it has a negative singularity and a vertical asymptote for $x \to 0^-$.

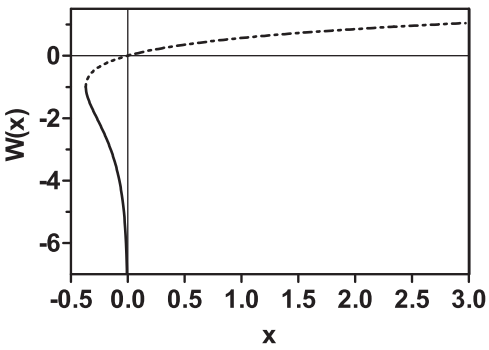

Fig. 1. The three real branches of the Lambert $W(x)$ function for the corresponding values of argument *x*. Region 1 (- · -) $x > 0$, region 2 (· · ·) $-\exp(-1) < x < 0$ and $0 > W(x) > -1$; region 3 (—) $-\exp(-1) < x < 0$ and $W(x) < -1$. Regions 1 and 2 divide the principal $W_0(x)$ branch as $W_0^+(x)$ and $W_0^-(x)$, respectively, while region 3 represents the lower $W_{-1}(x)$ branch.

The main properties and calculus of $W(x)$ are given in [5,7], but I present here a brief survey, and in particular the expressions for power series, derivatives and integrals of *W* are given in Appendix A.

3. Computing the Lambert *W* function

A specificity of the Lambert *W* function is that it is defined as an inverse function, and it cannot be expressed in terms of elementary mathematical functions. As a consequence, arbitrary precision evaluations can be obtained through iterative root-finding techniques. Numerous numerical methods are available for this purpose. The choice has to find the trade-off between complexity of implementation, conditions, and number of iterations to convergence at a given precision. These properties are usually controllable via the order of the method.

Newton's method [6,9] is a simple method with a second order in convergence that is appropriate, but with relatively slow convergence. The Newton iteration for Eq. (3) is available in the Supplementary Materials, provided by an initial guess of y_0, as described in [9]. However, near to the point $(-1, -\exp(-1))$, where the Lambert *W* function has a horizontal tangent, the Newton method only converges linearly, and can even fail to converge because of the cancellation errors in the denominator of Eq. (SM5) given in Supplementary Materials. Additionally, for *x* near, although below, zero, while the Newton method for $W_{-1}(x)$ is numerically stable, it can take many iterations to converge.

Hence, a better compromise is realized by the Halley method [5], which is a third-order method. This leads to high-precision evaluation in reasonable time. The Halley method is based on the iteration scheme given in Supplementary Materials, which is provided by an initial guess for y_0, as described in [5]. However, supplying this iteration technique with a sufficiently accurate first approximation of the order of 10^{-4} will give a machine-size floating-point precision of 10^{-16} in at least two iterations.

Furthermore, a fourth-order method was proposed in 1973 by Fritsch et al. [2], which is even faster, although it is also more complicated. Their algorithm 443 is based on an efficient iteration scheme and is also available in Supplementary Materials. This algorithm was superseded by algorithm 743 in 1995 [10].

The procedures described in this section are implemented in various technical mathematics software (e.g. Maplesoft Maple, Mathworks Matlab, Wolfram Mathematica). While the Lambert *W* function is simply called *W* in Maple and Matlab, in the

Mathematica computer algebra framework this function is built-in under the name of ProductLog.

4. Analytic approximations for the Lambert *W* function

Although the Lambert *W* function is useful in many scientific disciplines, it is not yet available in the standard mathematical software libraries that are also widely used in the life sciences. Hence, it is very interesting to express it approximately with other elementary mathematical functions that are readily available with any computer program. Thus, in this section, I will present such approximations for $W_{-1}(x)$ and $W_0(x)$ from [8], although some other approximations for $W_{-1}(x)$ have also been described over the last decade [11,12].

The upper branch of $W(x)$ can be broken into the two portions, and most applications are confined to either of these: $W_0^-(x)$ and $W_0^+(x)$. Therefore, Barry et al. [8] provided three simple analytical functions that can accurately approximate $W(x)$ for three different regions (see Fig. 1):

(a) Region 1, for $x \geq 0$: with the $W_0^{+*}(x)$ approximation to the positive principal branch $W_0^+(x)$, as in Eq. (6):

$$W_0^+(x) \approx W_0^{+*} = 1.45869 \cdot \ln\left(\frac{1.2 \cdot x}{\ln(2.4 \cdot x/(\ln(1+2.4 \cdot x)))}\right) - 0.45869 \cdot \ln\left(\frac{2 \cdot x}{\ln(1+2 \cdot x)}\right) \quad (6)$$

It should be noted here that for $x = 0$, the logarithmic terms in Eq. (6) are not defined, although when x tends to 0, both of these terms tend to the limit 0. Consequently, the $W_0^+(x)$ approaches 0 at $x = 0$. For the approximation of Eq. (6), the maximum relative error is below 0.2%.

(b) Region 2, for $-\exp(-1) \leq x < 0$: with the $W_0^{-*}(x)$ approximation to the negative principal branch $W_0^-(x)$, as in Eq. (7):

$$W_0^-(x) \approx W_0^{-*}(x) = -1 + \frac{\sqrt{2 \cdot (1+\exp(1) \cdot x)}}{\left(1 + ((N_1(x) \cdot \sqrt{2 \cdot (1+\exp(1) \cdot x)})/(N_2(x) + \sqrt{2 \cdot (1+\exp(1) \cdot x)}))\right)} \quad (7)$$

where

$$N_1(x) = \left(1 - \frac{1}{\sqrt{2}}\right) \cdot (N_2(x) + \sqrt{2}) \quad (8)$$

$$N_2(x) = 3\sqrt{2} + 6 - \frac{((2237 + 1457\sqrt{2}) \cdot \exp(1) - 4108\sqrt{2} - 5764)}{(215 + 199\sqrt{2}) \cdot \exp(1) - 430\sqrt{2} - 796} \cdot \sqrt{2 \cdot (1+\exp(1) \cdot x)} \quad (9)$$

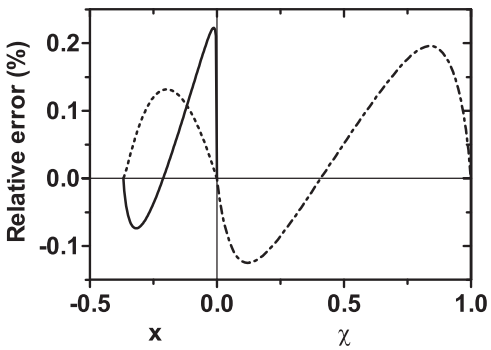

Fig. 2. Relative errors of the three different approximations of the Lambert *W* function. $W_0^{+*}(x)$ (- · -) for $x > 0$ on the exponential χ-scale, although on the linear x-scale: $W_0^{-*}(x)$ (· · ·) and $10 \times W_{-1}^{*}(x)$ (—) on the intervals $-\exp(-1) < x < 0$ and for $-\exp(-1) < x < 0$, respectively. The infinite x range interval $(0,\infty)$ has been mapped onto the interval (0,1) with the aid of the exponential χ-scale $\chi = 1 - 1/\ln(x + \exp(1))$.

The definition of $N_1(x)$ and $N_2(x)$ is taken so that the approximation of the $W_0^{-*}(x)$ is exact at $x = -\exp(-1)$ and 0, and the relative error of Eq. (7), the maximum of which is less than 0.15%, vanishes at these limits. Setting $N_1(x)$ and $N_2(x)$ in Eq. (7) gives the condensed expression of Eq. (10):

$$W_0^-(x) \approx W_0^{-*}(x) = -1 + \frac{\sqrt{2 \cdot (1+\exp(1) \cdot x)}}{(1 + (((3.4142 + 0.5799 \cdot \sqrt{2 \cdot (1+\exp(1) \cdot x)}) \cdot \sqrt{2 \cdot (1+\exp(1) \cdot x)})/(10.2426 + 2.9798 \cdot \sqrt{2 \cdot (1+\exp(1) \cdot x)})))} \quad (10)$$

(c) Region 3, for $-\exp(-1) \leq x < 0$: with the $W_{-1}^{*}(x)$ approximation to the lower branch $W_{-1}(x)$ with a maximum relative error of only 0.025%, as in Eq. (11):

$$W_{-1}(x) \approx W_{-1}^{*}(x) = \ln(-x) - 5.9506 \cdot \left(1 - \frac{1}{\left(1 + ((0.3361 \cdot \sqrt{-(1+\ln(-x))/2})/((1 + 0.0042 \cdot (1+\ln(-x))) \cdot \exp(-0.0201 \cdot \sqrt{-(1+\ln(-x))})))\right)}\right) \quad (11)$$

All of these three equations, Eqs. (6), (10) and (11), represent easily computable approximations for $W(x)$, with argument-x-depending relative errors as shown in Fig. 2. It should be noted here that the approximation equations Eqs. (6), (10) and (11) are constrained to give the correct values for W and the derivative dW/dx at the end points of their intervals. Consequently, the approximation equations are also continuous at the points $x = 0$ and $x = -\exp(-1)$.

5. Use of the Lambert *W* function in biochemical kinetics

The Lambert *W* function is nowadays mostly applied in computational sciences and mathematical physics [5], where it has been discussed in great detail. However, over the last decade, the use of the Lambert *W* function has broadened widely in chemical kinetics [13–16] and engineering [17–19]. In contrast, biochemistry and biotechnology are still seldom used to demonstrate the use of the Lambert *W* function, although biochemical kinetics provide the

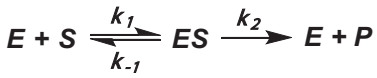

Scheme 1.

opportunity to apply it readily, as illustrated with the following three case problems.

5.1. Case I: classical and generalized Michaelis–Menten enzyme reaction systems

Traditionally, the kinetics of enzyme-catalyzed reactions have been described by the mechanism proposed by Henri [20], which can be schematically represented as illustrated in Scheme 1:

This is thus a reversible reaction between enzyme E and substrate S, giving the enzyme–substrate complex ES, which irreversibly yields product P. The rate equation that is associated with this mechanism was largely resolved by Michaelis and Menten [20], through the expression nowadays known as the Michaelis–Menten equation, as shown in Eq. (12):

$$v = -\frac{d[S]}{dt} = \frac{V \cdot [S]}{K_m + [S]} \tag{12}$$

where V is the limiting rate under saturation conditions, and K_m is the Michaelis constant. It should be noted that the latter two kinetic parameters can also be apparent (inhibitor-dependent) constants when the quantitative kinetics of inhibited enzyme-catalyzed reactions is studied in terms of the correlation between initial rate measurements according to the expression given in Eq. (12) [21]. However, this equation is of fundamental importance in enzyme kinetics for both theoretical and practical reasons, although little is known about its closed-form solution, which was reported for the first time by Beal in 1982 [3]. Fifteen years later, in 1997, Schnell and Mendoza [22] recognized that this solution can actually be expressed by the Lambert W function as:

$$[S]_t = K_m \cdot W_0\left\{\frac{[S]_0}{K_m} \cdot \exp\left(\frac{[S]_0 - V \cdot t}{K_m}\right)\right\} \tag{13}$$

Eq. (13) can be obtained from the widely known implicit integrated Michaelis–Menten equation [20], which can also be written as:

$$\frac{[S]_t}{K_m} + \ln\left(\frac{[S]_t}{K_m}\right) = \ln\left(\frac{[S]_0}{K_m}\right) + \frac{[S]_0 - V \cdot t}{K_m} \tag{14}$$

Substituting $y = [S]_t/K_m$ in Eq. (14) simplifies this to Eq. (15):

$$y + \ln(y) = \ln\left(\frac{[S]_0}{K_m} \cdot \exp\left(\frac{[S]_0 - V \cdot t}{K_m}\right)\right) \tag{15}$$

Eq. (15) shows similar relationships to those given in Eq. (1), with the identification of the closed-form solution, as in Eq. (16):

$$y = W_0\left\{\frac{[S]_0}{K_m} \cdot \exp\left(\frac{[S]_0 - V \cdot t}{K_m}\right)\right\} \tag{16}$$

Substituting for y in terms of $[S]_t$ and K_m results in Eq. (13), where the argument of W from Eq. (13) is positive at all times because K_m, $[S]_0$ and the exponential function are always positive. Therefore, a unique solution to Eq. (13) exists for any progress curve of interest when this solution to the basic Michaelis–Menten reaction mechanism is applied, as shown in Fig. 3. This algebraic integration approach is certainly the most appropriate, because enzyme-catalyzed reactions are typically presented in the form of time–concentration ($[S]_t$) measurements. Hence, time-course data analyses that use the integrated rate equations in its closed forms avoid the differentiation of concentrations into rates or computation of intensive numerical approaches for solving the rate equations in different forms (e.g. the Runge–Kutta integration and Newton–Raphson root-finding method for solving Eqs. (12) and (14), respectively).

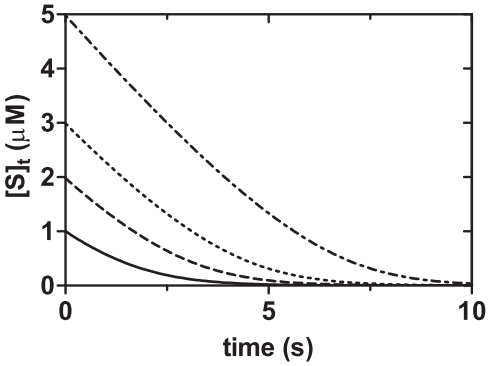

Fig. 3. Simulated progress curves of substrate concentrations for Michaelis–Menten-type (irreversible) enzyme-catalyzed reactions (V = 1 μM/s, K_m = 1 μM) with different initial substrate concentrations (1, 2, 3, 5 μM). The lines represent the data directly calculated from Eq. (13).

Scheme 2.

However, real-world enzymes generally do not obey the mechanism of Scheme 1, although the experimental conditions can sometimes be manipulated so that this is a very good approximation [20]. The forward velocities of many enzyme-catalyzed reactions are affected by product inhibition if the enzyme and product form an unproductive complex, EP, although more realistic reactions are also reversible. Thus, the sequence of elementary processes during the reaction involves two central complexes, ES and EP, that are mutually convertible at velocities that are characterized by the rate constants k_2 and k_{-2}, respectively, as illustrated in Scheme 2.

These kinetics of enzyme-catalyzed reactions presented in Scheme 2 are governed by the general Michaelis–Menten equation [20], as shown in Eq. (17):

$$v = \frac{d[P]}{dt} = -\frac{d[S]}{dt} = \frac{(V_f/K_f) \cdot [S] - (V_r/K_r) \cdot [P]}{1 + ([S]/K_f) + ([P]/K_r)} \tag{17}$$

V_f and K_f, and V_r and K_r, represent the limiting velocities and Michaelis constants in the forward and reverse directions, respectively. However, when such a reversible reaction is started with only the substrate and free enzyme, and when the free enzyme converts the substrate to product until it reaches its final equilibrium concentration $[S]_\infty$, the time-course of the reaction can be described by the closed-form solution [5], given as Eq. (18) (for its derivation, see Supplementary Materials):

$$[S]_t = [S]_0 - \Delta[S]_\infty + K_m^* \cdot W_0\left\{\frac{\Delta[S]_\infty}{K_m^*} \cdot \exp\left(\frac{\Delta[S]_\infty - V^* \cdot t}{K_m^*}\right)\right\} \tag{18}$$

where

$$\Delta[S]_\infty = \frac{(V_f \cdot [S]_0/K_f)}{(V_f/K_f + V_r/K_r)} = [S]_0 - [S]_\infty \tag{19}$$

$$V^* = \frac{(V_f/K_f + V_r/K_r)}{(1/K_f - 1/K_r)} \tag{20}$$

$$K_m^* = \frac{(1 + [S]_0/K_f)}{(1/K_f - 1/K_r)} - \Delta[S]_\infty \tag{21}$$

Eq. (18) is conceptually equal to Eq. (13), but the value of K_m^* depends on $[S]_0$ (see Eq. (21)). The solutions of Eq. (18) (i.e. the

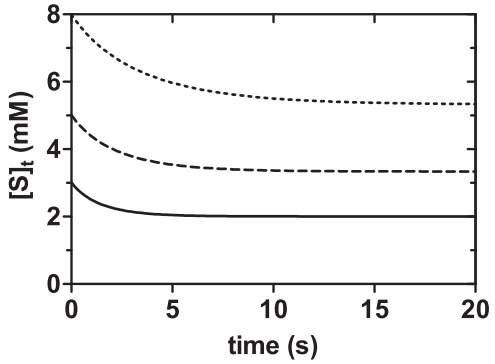

Fig. 4. Simulated progress curves of substrate concentrations for generalized Michaelis–Menten-type (reversible) enzyme-catalyzed reactions (V_f = 1 μM/s, V_r = 1 μM/s, K_f = 0.67 μM, K_r = 0.33 μM) with different initial substrate concentrations (3, 5, 8 μM). The lines represent the data directly calculated from Eq. (18).

values of $[S]_t$) at time zero and at times that tend to infinity are 0 and $[S]_\infty$, respectively (for details see Supplementary Materials). An interesting feature of Eqs. (20) and (21) is that V^* and K_m^* can have negative values if $K_f > K_r$, although they must both have the same sign. Additionally, Eq. (18) indicates that argument x in this equation can be either positive (when $K_f < K_r$) or negative (when $K_f > K_r$), as $\Delta[S]_\infty$ in Eq. (19) is always positive, while the sign of K_m^* depends on the relationship between K_f and K_r. Nevertheless, whether argument x is positive or negative, the required solution to Eq. (18) as shown in Fig. 4 is from the principal branch of the Lambert W function; i.e. $W_0(x) \geq -1$ [5,23].

Eqs. (13) and (18) have been used for progress-curve analyses for enzyme and microbial kinetic reactions that apply powerful mathematical software with a built-in W function [22–25]. Unfortunately, the standard software libraries that are most widely used in the life sciences are not set up to handle equations that involve the W function. To avoid this problem, the replacement of the integrated Michaelis–Menten equation with an empiric integrated 1 − exp alternative model equation was proposed recently by Keller et al. [26], although this reformulation causes a distortion in the Michaelis constant and deviations between both integrated model solutions can increase significantly with time [27]. However, it is known now that the replacement of model equations is not necessary at all, as the use of approximations to the Lambert W function has been recommended recently for those who use standard computer programs without implemented W code [27–29].

5.2. Case II: Michaelis–Menten enzyme reaction systems with endogenous substrate production

There are many exceptional biological kinetics systems that cannot be described by only the classical Michaelis–Menten equation; e.g. sediments, anaerobic digestor sludge, and rumen fluid [30–32]. In these systems, the substrate being consumed is also endogenously produced, and hence Eq. (22) must be modified to include an additional parameter R, as:

$$v = \frac{d[S]}{dt} = -\frac{V \cdot [S]}{K_m + [S]} + R \tag{22}$$

where R is the rate of endogenous substrate production. Robinson and Characklis [31] published an implicit integral form of Eq. (22) in 1984, although Goudar recently identified an error in that equation [33] and re-derived. The complete closed-form analytical solution of this equation [53] which has remained unnoticed since its first use in 2007 [34].

The solutions of this modified Michaelis–Menten rate equation (see Eq. (22)) under the particular initial conditions depend on

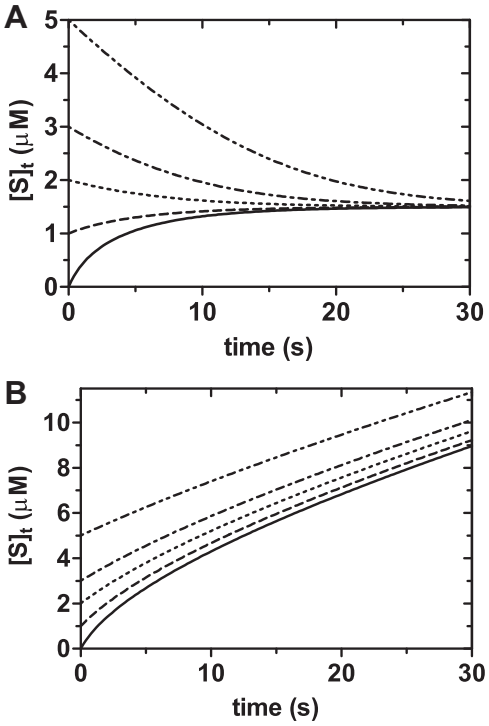

Fig. 5. Simulated progress curves of substrate concentrations for Michaelis–Menten-type enzyme-catalyzed reactions (V = 1 μM/s, K_m = 1 μM) in systems with different initial substrate concentrations (0, 1, 2, 3, 5 μM) and various endogenous rates of substrate production. The lines represent the data directly calculated from Eq. (23), with respect to two different cases: (A) with $R > V$ (R = 1.1 μM/s) when Eq. (23) is expressed with the lower branch W_{-1} of the Lambert W function and (B) with $R < V$ (R = 0.6 μM/s) when Eq. (23) is expressed with the principal branch W_0 of the Lambert W function.

factor b, which denotes the difference between the rate parameters R and V_{max} ($b = R - V_{max}$), as shown in Eq. (23) [35]:

$$[S]_t = \begin{cases} -\dfrac{R \cdot K_m}{b} - \dfrac{V \cdot K_m}{b} \cdot W_{-1}[x(t)], & b > 0 \\ -K_m + \sqrt{(K_m + [S]_0)^2 + 2 \cdot V \cdot K_m \cdot t}, & b = 0 \\ -\dfrac{R \cdot K_m}{b} - \dfrac{V \cdot K_m}{b} \cdot W_0[x(t)], & b < 0 \end{cases} \tag{23}$$

where $x(t)$ represents the time-dependent argument of this function, as expressed as in Eq. (24):

$$x(t) = -\frac{(R \cdot K_m + b \cdot [S]_0)}{V \cdot K_m} \cdot \exp\left(-\frac{(R \cdot K_m + b \cdot [S]_0 + b^2 \cdot t)}{V \cdot K_m}\right) \tag{24}$$

Eq. (24) indicates that the argument of the Lambert W function has a limit, $\lim_{t \to \infty} x(t) = 0$, although $x(t)$ is negative ($-\exp(-1) < x < 0$) for $b > 0$ (i.e. $R > V$) at all times, as the initial concentration $[S]_0$, the Michaelis constant K_m, the rates R and V, and the exponential function are always positive. This is in agreement with the solution of Eq. (23), which is expressed via $W_{-1}(x)$, which is defined only for the interval $[-\exp(-1),0)$. Thus, for $b > 0$, the progress curves always increase with time, as shown in Fig. 5B, although simultaneously the slopes of these progress curves decline and approach the limit b ($= R - V$). However, for $b < 0$ (i.e. $R < V$), x(t) can be either negative (for the interval $[-\exp(-1),0)$) or positive (for the interval $[0,\infty)$). The sign of x depends on the following relationships: (i) if $R > V \cdot [S]_0/(K_m + [S]_0)$, then x is negative and the progress curves increase; and (ii) if $R < V \cdot [S]_0/(K_m + [S]_0)$, then x is positive and the progress curves decrease. However, in both cases, the solutions of the model Eq. (23) asymptotically approach the steady-state concentration $[S]^* = -R \cdot K_m/(R - V)$, as shown in Fig. 5A, when $R < V$. Simultaneously the slopes of these progress curves are negative or

Scheme 3.

positive, although they flow together to zero when steady-state is attained.

The closed-form solution of Eq. (22) has been used for progress-curve analysis for describing one-compartment pharmacokinetics model with constant drug input [34], although recently, the appropriate substitution with approximations to the Lambert *W* function were suggested [35].

5.3. Case III: kinetics of analyte binding to the surface by mass-transport limitation

In a typical experiment using surface plasmon resonance detection, a selective surface is created by covalent immobilization of a specific ligand to a surface of a sensor chip. A sample (analyte) solution is then injected at a constant flow rate and the molecules of analyte bind with noncovalent interactions to the surface ligand over time. The response signal detected is based on the changes of refractive index, which are proportional to the level of accumulation of mass at the binding surface [36]. However, during sample injection, the analyte concentration at the surface is lower than in the bulk flow, as a consequence of mass-transport limitations. Thus, a simple model based on this assumption was proposed by Myzska et al. [37], where the observed binding is treated as a two-step process, as shown in Scheme 3.

This two-step process represents transport of the analyte to the surface (first step), followed by a binding interaction with the immobilized ligand (second step). This has been termed the two-compartment model.

Within the two-compartment model, the binding kinetics of the association phase as shown in Fig. 6 (where the analyte bulk concentration is kept constant by a continuous injection of fresh analyte solution at a constant flow rate) can be described in the steady-state approximation by the following nonlinear differential equation [38,39]:

$$\frac{dR}{dt} = k_a \cdot (R_{\max} - R) \cdot \left(\frac{[A]_0 + k_d \cdot R/k_m}{1 + k_a \cdot (R_{\max} - R)/k_m} \right) - k_d \cdot R \qquad (25)$$

In Eq. (25), k_a ($M^{-1}\,s^{-1}$) and k_d (s^{-1}) are the association and dissociation rate constants, respectively; $[A]_0$ (M) is the initial analyte concentration; R_{max} and R are the maximum and current response intensities expressed in response units (RU), and K_m ($RU\,M^{-1}\,s^{-1}$) is the phenomenological mass-transport constant. For the initial condition $R(0) = 0$, the analytical solution of Eq. (25) in the closed-form reading is as follows:

$$R(t) = R_\infty \cdot \left(1 - \frac{W_0(\alpha \cdot \exp(\alpha - \beta \cdot t))}{\alpha} \right) \qquad (26)$$

where

$$R_\infty = \frac{R_{\max} \cdot [A]_0}{(K_D + [A]_0)} \qquad (27)$$

$$\alpha = \frac{k_a \cdot [A]_0 \cdot R_{\max}}{k_d \cdot R_{\max} + k_m \cdot (K_D + [A]_0)} \qquad (28)$$

$$\beta = \frac{k_a \cdot [A]_0 + k_d}{(1 + (k_d \cdot R_{\max}/(k_m \cdot (K_D + [A]_0))))} \qquad (29)$$

Furthermore, it should be noted that ligand equilibrium dissociation constants from surfaces are defined as the ratio between the dissociation and association rate constants ($K_D = k_d/k_a$).

In the dissociation phase, the differential equation still holds, although since $[A]_0 = 0$, it follows that the analytical closed-form solution in this case is:

$$R(t) = -\gamma \cdot W_0 \left(-\frac{R_0}{\gamma} \cdot \exp\left(\frac{-k_a \cdot R_0 - k_m \cdot k_d \cdot (t - t_0)}{k_a \cdot \gamma} \right) \right) \qquad (30)$$

where

$$\gamma = \frac{k_a \cdot R_{\max} + k_m}{k_a} \qquad (31)$$

and $R = R_0$ at time t_0, which is the start of the dissociation phase. It should be noted that there are negative signs in Eq. (30), although the argument to *W* in the equation always lies between $-\exp(-1)$ and zero whenever $t > t_0$, implying that the Lambert *W* function is defined and negative here. The negative sign at the start of Eq. (30) then makes the total value of this expression positive (see Fig. 6).

As Eq. (25) takes into consideration the entire processes of mass transport and binding kinetics in the solution, Eqs. (26) and (30) present the complete analytical solutions that allow both determination of the active concentrations and accurate and precise measurements of the association and dissociation rate constants of the binding interactions from response curves (see Fig. 6). The main advantage of these solutions is that global progress-curve analysis explicitly shows the reliability of the results.

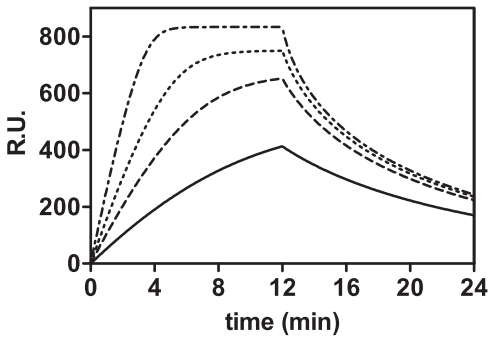

Fig. 6. Simulated response curves for analyte binding kinetics to the surface by mass-transport limitation ($k_a = 1.8 \times 10^6\,M^{-1}\,min^{-1}$, $k_d = 0.18\,min^{-1}$, $k_m = 9 \times 10^6\,RU\,M^{-1}\,min^{-1}$, $R_{max} = 1000\,RU$) in system with different initial analyte concentrations (100, 200, 300, 500 nM). The ascending and descending lines represent the data directly calculated from Eqs. (26) and (30), respectively.

6. Other uses of the Lambert *W* function in engineering and life sciences

Although this review is mainly focused on problems considering the Lambert *W* function that appear in the biochemical and biotechnological disciplines [22–29,34–39], and in chemical engineering [13–19], other applications of *W* of practical import have been discovered in various engineering and life sciences, and I cite here only recently published literature. Thus, *W* appears in solutions to a large family of equations that describes situations in physiology [40,41], hydrology [42,43], colloid and interface science [44,45], materials and transport research [46–48], electrochemistry [49], and droplet microfluidics [50]. Furthermore, many delay differential equations, where the present rate of change in some quantity depends on the value of the quantity at an earlier moment, can be solved in terms of *W* (see [51] and references therein). The equations of this kind can be frequently found in population dynamics, economics, and control theory, although these fields are not within the scope and interests of the readers of this journal.

7. Conclusion

In this review, I have presented some of the calculus properties of the Lambert *W* function, along with its numerical evaluation

and the approximation functions to $W(x)$. I have combined these with some biochemical kinetics examples of its applications and the available references on this function. Furthermore, I believe that awareness of the Lambert W function in the fields of biochemistry and biotechnology will also increase in the years to come [15,52], and many more applications will be recognized in these scientific disciplines. Consequently, the aim of this article is to facilitate this process, which will help in the identification of the practical aspects of the Lambert W function for the life-sciences research community.

Acknowledgment

This work was supported by the Slovenian Research Agency (grant P1-170).

Appendix A.

The principal branch of W is analytical at $x = 0$, and its power series expression about the origin can be given as:

$$W_0(x) = \sum_{n\geq 1} (-n)^{n-1} \frac{x^n}{n!} \tag{A1}$$

The radius of convergence of this series is equal to $\exp(-1)$ where $|W(x)| < 1$.

The rules for integration and differentiation of W are as follows:

$$\int W(x)dx = x \cdot \left(W(x) - 1 + \frac{1}{W(x)} \right) + C \tag{A2}$$

$$W'(x) = \frac{W(x)}{x \cdot (1 + W(x))} \tag{A3}$$

where Eq. (A3) is valid for $x \neq 0$. At zero, the derivative is defined in the form of the limit:

$$\lim_{x\to 0} W_0'(x) = 1 \tag{A4}$$

Appendix B. Supplementary data

Supplementary data associated with this article can be found, in the online version, at doi:10.1016/j.bej.2012.01.010.

References

[1] E.M. Wright, Solution of the equation $z\exp(z) = a$, Proc. R. Soc. Edinb. A 65 (1959) 193–203.
[2] F.N. Fritsch, R.E. Shafer, W.P. Crowley, Algorithm 443: solution of the transcendental equation $we^w = x$, Commun. AMC 16 (1973) 123–124.
[3] S.L. Beal, On the solution to the Michaelis–Menten equation, J. Pharmacokinet. Biopharm. 10 (1982) 109–119.
[4] R.M. Corless, G.H. Gonnet, D.E.G. Hare, D.J. Jeffrey, Lambert's W function in Maple, Maple Tech. Newslett. 9 (1993) 12–22.
[5] R.M. Corless, G.H. Gonnet, D.E.G. Hare, D.J. Jeffrey, D.E. Knuth, On the Lambert W function, Adv. Comput. Math. 5 (1996) 329–359.
[6] S.L. Beal, Computation of the explicit solution to the Michaelis–Menten equation, J. Pharmacokinet. Biopharm. 11 (1983) 641–657.
[7] S.R. Valluri, D.J. Jeffrey, R.M. Corless, Some applications of the Lambert W function to physics, Can. J. Phys. 78 (2000) 823–831.
[8] D.A. Barry, J.Y. Parlange, L. Li, H. Prommer, C.J. Cunningham, F. Stagnitti, Analytical approximations for real values of the Lambert W-function, Math. Comput. Simul. 53 (2000) 95–103.
[9] W. Gautschi, The Lambert W-function and some of their integrals: a case study of high-precision computation, Numer. Algor. 57 (2011) 27–34.
[10] D.A. Barry, S.J. Barry, P.J. Culligan-Hensley, Algorithm 743: a Fortran routine for calculating real values of the W-function, ACM Trans. Math. Softw. 21 (1995) 172–181.
[11] J.Y. Parlange, D.A. Barry, R. Haverkamp, Explicit infiltration equations and the Lambert W-function, Adv. Water Resour. 25 (2002) 1119–1124.
[12] D.A. Barry, J.Y. Parlange, L. Li, D.S. Jeng, M. Crapper, Green-Ampt approximations, Adv. Water Resour. 28 (2005) 1003–1009.
[13] I.A. Vinokurov, J. Kankare, Kinetics of multilayer Langmuirian adsorption, Langmuir 18 (2002) 6789–6795.
[14] G.S. Yablonsky, D. Constales, G.B. Marin, Coincidences in chemical kinetics: surprising news about simple reactions, Chem. Eng. Sci. 65 (2010) 6065–6076.
[15] B.W. Williams, The utility of the Lambert function $W[a\exp(a - bt)]$ in chemical kinetics, J. Chem. Educ. 87 (2010) 647–651.
[16] B.W. Williams, Alternate solutions for two particular third order kinetic rate laws, J. Math. Chem. 49 (2011) 328–334.
[17] J.R. Sonnad, C.T. Goudar, Explicit reformulation of the Colebrook–White equation for turbulent flow friction factor calculation, Ind. Eng. Chem. Res. 46 (2007) 2593–2600.
[18] D. Clamond, Efficient resolution of Colebrook equation, Ind. Eng. Chem. Res. 48 (2009) 3665–3671.
[19] K. Sun, A. Kasperski, Y. Tian, L. Chen, New approach to the nonlinear analysis of a chemostat with impulsive state feedback control, Int. J. Chem. React. Eng. 8 (2010) A99.
[20] I.H. Segel, Enzyme Kinetics, John Wiley & Sons, New York, 1993.
[21] A. Bavec, A. Juréus, B. Cigić, Ü. Langel, M. Zorko, Peptitergent PD_1 affects the GTPase activity of rat brain cortical membranes, Peptides 20 (1999) 177–184.
[22] S. Schnell, C. Mendoza, Closed-form solution for time-dependent enzyme kinetics, J. Theor. Biol. 187 (1997) 207–212.
[23] C.T. Goudar, J.R. Sonnad, R.G. Duggleby, Parameter estimation using a direct solution of the integrated Michaelis–Menten equation, Biochim. Biophys. Acta 1429 (1999) 377–383.
[24] C.T. Goudar, T.G. Ellis, Explicit oxygen concentration expression for estimating extant biodegradation kinetics from respirometric experiments, Biotechnol. Bioeng. 75 (2001) 74–81.
[25] C.T. Goudar, S.K. Harris, M.J. McInerney, J.M. Suflita, Progress curve analysis for enzyme and microbial kinetic reactions using explicit solutions based on the Lambert W function, J. Microbiol. Methods 59 (2004) 317–326.
[26] F. Keller, B. Hartmann, D. Czock, Explicit solution of the integrated $1 - \exp$ equation for predicting accumulation and decline of concentrations for drugs obeying nonlinear saturation kinetics, Ther. Drug Monit. 31 (2009) 783–785.
[27] M. Goličnik, An alternative explicit model expression equivalent to the integrated Michaelis–Menten equation and its application to nonlinear saturation pharmacokinetics, Ther. Drug Monit. 33 (2011) 362–365.
[28] M. Goličnik, Explicit analytic approximations for time-dependent solutions of the generalized integrated Michaelis–Menten equation, Anal. Biochem. 411 (2011) 303–305.
[29] M. Goličnik, Evaluation of enzyme kinetic parameters using explicit analytic approximations to the solution of the Michaelis–Menten equation, Biochem. Eng. J. 53 (2011) 234–238.
[30] J.A. Robinson, J.M. Tiedje, Kinetics of hydrogen consumption by rumen fluid, anaerobic digestor sludge, and sediment, Appl. Environ. Microbiol. 44 (1982) 1374–1384.
[31] J.A. Robinson, W.G. Characklis, Simultaneous estimation of V_{max}, K_m and the rate of endogenous substrate production R from substrate depletion data, Microb. Ecol. 10 (1984) 165–178.
[32] H.B. Nielsen, Z. Mladenovska, B.K. Ahring, Kinetics of propionate conversion in anaerobic continuously stirred tank reactors, Environ. Technol. 29 (2008) 151–160.
[33] C.T. Goudar, Accurate kinetic parameter estimation during progress curve analysis of systems with endogenous substrate production, Biotechnol. Bioeng. 108 (2011) 2499–2503.
[34] S. Tang, Y. Xiao, One-compartment model with Michaelis–Menten elimination kinetics and therapeutic window: an analytical approach, J. Pharmacokinet. Pharmacodyn. 34 (2007) 807–827.
[35] M. Goličnik, Explicit reformulations of the Lambert W-omega function for calculations of the solutions to one-compartment pharmacokinetic models with Michaelis–Menten elimination kinetics, Eur. J. Drug Metab. Pharmacokinet. 36 (2011) 121–127.
[36] L.L.H Christensen, Theoretical analysis of protein concentration determination using biosensor technology under conditions of partial mass transport limitation, Anal. Biochem. 249 (1997) 153–164.
[37] D.G. Myszka, M. Morton, L. Doyle, I.M. Chaiken, Kinetic analysis of protein antigen–antibody interaction limited by mass transport on an optical biosensor, Biophys. Chem. 64 (1997) 127–137.
[38] K. Sigmundsson, G. Masson, R. Rice, N. Beauchemin, B. Öbrink, Determination of active concentrations and association and dissociation rate constants of interacting biomolecules: an analytical solution to the theory for kinetic and mass transport limitations in biosensor technology and its experimental verification, Biochemistry 41 (2002) 8263–8276.
[39] W. Kusnezow, Y.V. Syagailo, S. Rüffer, K. Klenin, W. Sebald, J. Hoheisel, C. Gauer, I. Goychuk, Kinetics of antigen binding to antibody microspots: strong limitations by mass transport to the surface, Proteomics 6 (2006) 794–803.
[40] R.D. Simitev, V.N. Biktashev, Asymptotic of conduction velocity restitution in models of electrical excitation in the heart, Bull. Math. Biol. 73 (2011) 72–115.
[41] A.E. Ehret, M. Böl, M. Itskov, A continuum constitutive model for the active behavior of skeletal muscle, J. Mech. Phys. Solids 59 (2011) 625–636.
[42] F. Heße, F.A. Radu, M. Thullner, S. Attinger, Upscaling of the advection-diffusion-reaction equation with Monod reaction, Adv. Water Resour. 32 (2009) 1336–1351.
[43] R. Gong, C. Lu, W.M. Wu, H. Cheng, B. Gu, D. Watson, P.M. Jardine, S.C. Brooks, C.S. Criddle, P.K. Kitanidis, J. Luo, Estimating reaction rate coefficients within a travel-time modeling framework, Groundwater 49 (2011) 209–218.

[44] N. Fries, M. Dreyer, An analytical solution of capillary rise restrained by gravity, J. Colloid Interface Sci. 320 (2008) 259–263.
[45] M. Hilpert, Explicit analytical solutions for liquid infiltration into capillary tubes: dynamic and constant contact angle, J. Colloid Interface Sci. 344 (2010) 198–208.
[46] L. Zhang, D. Xing, J. Sun, Calculating activation energy of amorphous phase with the Lambert *W* function, J. Therm. Anal. Calorim. 100 (2010) 3–10.
[47] M. Conrath, N. Fries, M. Zhang, M.E. Dreyer, Radial capillary transport from an infinite reservoir, Transp. Porous Media 84 (2010) 109–132.
[48] C.H. Belgacem, M. Fnaiech, Solution for the critical thickness models of dislocation generation in epitaxial thin films using the Lambert *W* function, J. Mater. Sci. 46 (2011) 1913–1915.
[49] A. Pohjoranta, A. Mendelson, R. Tenno, A copper electrolysis cell model including effects of the ohmic potential loss in the cell, Electrochim. Acta 55 (2010) 1001–1012.
[50] J. Berthier, P. Silberzan, Microfluidics for Biotechnology, Artech House, Norwood, 2010.
[51] S. Yi, P.W. Nelson, A.G. Ulsoy, Time Delay Systems: Analysis and Control Using the Lambert *W* Function, World Scientific, London, 2010.
[52] M. Goličnik, Exact and approximate solutions for the decades-old Michaelis–Menten equation: progress-curve analysis through integrated rate equations, Biochem. Mol. Biol. Educ. 39 (2011) 117–125.
[53] C.T. Goudar, An explicit solution for progress-curve analysis in systems characterized by endogenous substrate production, Microb. Ecol. (in press) doi:10.1007/s00248-011-9996-3.